RSC Advances

ROYAL SOCIETY OF CHEMISTRY

www.rsc.org/advances

Carboxymethyl gum katira: Synthesis, characterization and evaluation for nanoparticulate drug delivery

Minkal, Munish Ahuja*, D C Bhatt

Drug Delivery Research Laboratory, Department of Pharmaceutical Sciences, Guru Jambheshwar University of Science and Technology, Hisar-125 001, India

* Corresponding author:
Dr Munish Ahuja,
Drug Delivery Research Laboratory,
Department of Pharmaceutical Sciences,
G.J.University of Science and Technology, Hisar 125 001, India
E-mail address: munishahuja17@yahoo.co.in
Tel: +91-1662-263515
Fax: +91-1662-276240

Abstract

In the present study carboxymethyl derivative of gum katira was synthesized and explored for drug delivery applications. Carboxymethyl functionalization was achieved by reacting it with monochloroacetic acid under alkaline conditions. The modified gum was found to have degree of carboxymethyl substitution of 0.6. Carboxymethyl modification was confirmed by FT-IR study. Thermal studies revealed higher thermal stability, while X-ray diffraction pattern showed increase in crystallinity of carboxymethyl derivative. SEM study showed that carboxymethylation changes thin flaky, smooth surface particles into polyhedral sharp edged particles with rough surface. Further, the preparation of polyelectrolyte complex nanoparticles of carboxymethyl gum katira and chitosan was optimized using 2-factor, 3-level central composite experimental design. The optimal calculated parameters were concentrations of carboxymethyl gum katira (0.26%, w/v) and chitosan (0.03%, w/v), which provided polyelectrolyte nanoparticles of size 269 nm and ofloxacin entrapment of 83.65%. The nanosuspension was found to release 92% of ofloxacin in 24h, following Higuchi's release kinetics with the mechanism of release being Super Case-II transport. An ophthalmic nanosuspension of ofloxacin (0.3%,w/v) formulated using the optimized batch showed slightly higher apparent corneal permeability of ofloxacin than the aqueous solution of ofloxacin across the isolated porcine cornea. Further, the histological studies on corneas treated with ophthalmic nanosuspension revealed corneal biocompatibility. In conclusion carboxymethyl gum katira possess an excellent potential for exploring polyelectrolyte nanoparticulate ocular drug delivery.

1. Introduction

Natural gums, resins, mucilages and latex are the plant secretions that are being extensively used in food, cosmetics, pharmaceutical, textile and leather industries because of their easy availability, low cost, biocompatibility and biodegradability[1], but their applications are limited due to uncontrolled hydration, microbial contamination, pH dependent solubility and changes in viscosity during storage. A variety of physical and chemical methods have been employed to improve the properties of the natural gums for their application in the biological systems[2]. Carboxymethylation is among one of the various strategies used for functionalization of natural polymers[3]. It is widely employed modification approach because of its ease of processing, lower cost of chemicals and versatility of the product. Carboxymethyl derivatives usually have better aqueous solubility. Carboxymethylation of chitosan[4], cellulose[5] guar[6,7], dextran[8], and gellan gum[9], gum kondagogu[10], kappa-carrageenan[11], xanthan[12]have earlier been carried out to enhance the solubility of these polymers in water.

Gum katira, is an exudate from the fibrous bark of *Cochlospermum religiosum*, a softwood tree of the family Cochlospermaceae[13]. The gum is insoluble in water which swells in water to form a transparent pasty mass. The gum is sweet, thermogenic, anodyne, sedative and useful in cough, diarrhea, dysentery, pharyngitis, gonorrhea, syphilis and trachoma[14]. The gum is extensively used in the cigar, paste, and ice-cream industry and has been successfully used as a gelling agent in tissue culture media. Chemical structure of gum katira comprises of L-rhamnose, D-galactose and D-galacturonic acid in a molar ratio 3 : 2 : 1, respectively, with traces of a ketohexose[15]. A review of literature showed that gum katira has been evaluated for the colon targeted drug delivery[16] and as release rate modifier in the matrix tablets[17]. Gum katira was also employed as reducing and stabilizing agent for green synthesis of gold nanoparticles.[18]

In present study, carboxymethyl functionalization of gum katira was carried out. The modified gum katira was characterized by FT-IR, thermal, X-ray diffraction and SEM studies. Further, its interaction with cationic chitosan was optimized using 2-factor, 3-level central composite experimental design to prepare polyelectrolyte nanoparticles with optimum particle size and entrapment of ofloxacin, a model drug. The optimized batch was further formulated into ophthalmic nanosuspension of ofloxacin (0.3%, w/v) and evaluated comparatively with conventional commercial ofloxacin ophthalmic solution (0.3%, w/v) for corneal permeation characteristics using isolated porcine cornea. Toxicological profile of ophthalmic nanosuspension was studied by conducting histological studies of exposed corneas.

2. Materials and methods

2.1 Materials

Gum katira was purchased from the local market of Hisar. Ofloxacin was obtained as gift sample from Ranbaxy Research Laboratory (Gurgaon, India). Monochloroacetic acid was purchased from Hi-Media Lab. Pvt. Ltd. (Mumbai, India). Sodium hydroxide, methanol and glacial acetic acid were procured from Sisco Research Laboratory (Mumbai, India). Whole eye balls of pig were procured from the local slaughter house (Hisar, India). All other chemicals used were of reagent grade, and were used as received.

2.2 Synthesis of carboxymethyl gum katira

Carboxymethylation of gum katira was carried out employing monochloroacetic acid[19]. Gum katira (1 g) was dispersed in 80 ml of ice cold sodium hydroxide solution (45%, w/w) with the aid of stirring for 30 min, followed by addition of 10 ml of monochloroacetic acid solution (75%, w/v) under constant stirring. The reaction mixture was then heated to 70 ◦C under constant stirring for 30 min, cooled and suspended into 80% (v/v) methanol. The precipitates so obtained

were filtered and washed with glacial acetic acid till washings were neutral. The product so obtained, was washed three times with 60 ml portions of 80% (v/v) methanol, filtered and dried in an oven at 40 ◦C.

2.3. Characterization of carboxymethyl gum katira

Degree of carboxymethyl substitution

The degree of carboxymethyl substitution was assessed by employing classical acid wash method[20]. In brief, 2 g of freshly precipitated carboxymethyl gum katira was dispersed in 100 ml of hydrochloric acid reagent, in 250 ml Erlenmeyer flask for 3–4 h. Carboxymethyl gum katira was filtered and washed with 70% methanol till the washings were neutral to methyl red followed by drying to constant weight in an oven at 80 ◦C. Dried carboxymethyl gum katira (500 mg) was dispersed in 70% methanol (10 ml) in Erlenmeyer flask and stirred for 30 min. To this an aliquot of 50 ml of distilled water and 15 ml of 0.5N sodium hydroxide was added and stirred for 3 h to dissolve the sample completely. The excess of sodium hydroxide was back titrated employing 0.5N hydrochloric acid as titrant and phenolphthalein as an indicator.

The degree of carboxymethyl substitution (DS) of carboxymethyl gum katira was calculated using the following equation:

$$DS = \frac{0.162\ A}{1-0.058A} \quad \ldots\ldots\ldots\ldots\ldots\ldots\ldots\ldots\ldots\ldots\ldots\ldots (1)$$

where, A is the miliequivalents of sodium hydroxide required per gram of the sample.

FT-IR spectroscopy

The samples of gum katira and carboxymethyl gum katira were subjected to FT-IR spectroscopy in a Fourier-transform infrared spectrophotometer (IR Affinity, Shimadzu) in range of (4000 cm^{-1} to 400 cm^{-1}) as KBr pellet.

Thermal analysis

Differential scanning calorimetric thermograms of gum katira and carboxymethyl gum katira were recorded using differential scanning calorimeter (Q10, TA Systems, USA) in the temperature range of (40–600 ◦C) at a heating rate of 10 ◦C per minute in nitrogen atmosphere.

X-ray diffractometry

X-ray diffractogram of gum katira and carboxymethyl gum katira samples were recorded employing X-ray diffractometer (Bruker Focus D8). The sample powders were scanned from 0^o to 70^o diffraction angle (2θ) range under the following measurement conditions: source, nickel filtered Cu-Kα radiation; voltage 35 kV; current 25 mA; scan speed 0.05 min^{-1}.

Scanning electron microscopy

Gum katira and carboxymethyl gum katira samples were coated with gold and mounted in a sample holder. The photomicrographs of samples were taken at an accelerating voltage of 10 kV at different magnifications. (JEOL, JSM-6100).

Viscosity

Viscosity of 2% (w/v) dispersions of gum katira and carboxymethyl gum katira was determined using Brookfield viscometer (Model RVDVE 230, Brookfield Engineering Laboratories, Middleboro, USA) using spindle number 5 at different shear rates.

2.4 Evaluation of carboxymethyl gum katira for nanoparticulate drug delivery

Carboxymethyl gum katira was found to interact with chitosan forming polyelectrolyte complexes. This interaction was explored for formulating polyelectrolyte nanoparticulate delivery system using ofloxacin as a model drug.

2.4.1 Preparation of carboxymethyl gum katira-chitosan polyelectrolyte nanoparticles

An aqueous solution of carboxymethyl gum katira (0.10-0.40%,w/v) containing ofloxacin (50%, w/w of the gum) was added drop by drop under sonication (Power Sonic 405) to the chitosan solution (0.03-0.05%, w/v) in acetic acid (2% v/v). The nanosuspension was further probe sonicated for 15 min. (Q55, Qsonica USA**)**

Optimization of carboxymethylated gum katira nanoparticles was done using a central composite design with $\alpha = 1$ as per standard protocol. The various preliminary trials were carried out to select the formulation variables. Concentrations of carboxymethyl gum katira (X_1) and chitosan (X_2) were varied and factor levels were suitably coded. All other formulation and process variables were kept constant. Particle size and entrapment efficiency were considered as response variables. Design Expert Software (Version 8.0.4, Stat-Ease Inc., Minneapolis, MN) was used for statistical analysis and design of experiment.

2.4.2 Characterization of ofloxacin-loaded carboxymethyl gum katira- chitosan polyelectrolyte nanoparticles

Particle size

Dynamic light scattering was used to determine the particle size of nanosuspension. One milliliter of nanosuspension was analyzed in disposable sizing cuvette at 25ºC with an equilibration time of 120s and number of runs in an automatic mode; in particle size analyzer (Zetasizer Nano ZS90, Malvern, UK).

Entrapment efficiency

For the determination of entrapment efficiency, nanosuspension was centrifuged (Cooling centrifuge, 4K-15, Sigma, Germany) at 18000 rpm for 20 min at 4ºC. Supernatant was analyzed spectrophotometrically (UV spectrophotometer Carry) for free ofloxacin at 290 nm. Entrapment efficiency (%) was calculated by the formula given below:

$$\%\, Entrapment\ efficiency = \frac{(Oft - Ofu)}{(Oft)} \times 100 \ldots\ldots\ldots\ldots\ldots\ldots \quad (2)$$

Where, Of_t – Total ofloxacin, Of_u – unbound ofloxacin

Morphology

Morphology of optimized batch of ofloxacin-loaded carboxymethyl gum katira nanoparticles was observed by transmission electron microscopy (TEM). A drop of nanosuspension was loaded onto a copper grid with excess solution soaked using a blotting paper. The grid was air dried and loaded in the goniometer of the instrument for viewing. TEM micrograph was captured at 200 kV accelerating voltage.

In vitro drug release

In vitro release of ofloxacin from the optimized batch of carboxymethyl gum katira–chitosan nanoparticles was studied by dialysis sac method[21]. Dialysis sac (cut off 10 kDa) containing 3 ml of nanoparticulate formulation or ofloxacin solution was tied with thread to the paddle of USP type II dissolution apparatus (TDT-08L, Electrolab, India) . The paddle was then immersed in 200 ml of release media (0.1 M HCl) maintained at 37±0.5^{o}C and was rotated at the speed of 50 rpm. Sample aliquots of 5 ml were withdrawn at regular intervals and the volume of the medium was maintained by adding equal volumes of fresh media. The contents of ofloxacin in the samples were determined spectrophotometrically by measuring the absorbance at 290 nm.

Antimicrobial Study

Antimicrobial activity of ofloxacin (0.13%, w/v) loaded carboxymethyl gum katira–chitosan nanoformulation was comparatively evaluated with the standard ofloxacin solution (0.13%, w/v) employing agar diffusion method by measuring the zone of inhibitions produced by the test formulations against *Escherichai coli, Staphylococcus auereus* and *Psuedomonas aeruginosa*. A suspension of the microbial strains diluted to 10^4CFU/ml was inoculated on the agar plates, and 100 µl of the test formulation was applied in the central cavity of the agar plates. The plates were incubated at 37 ± 0.5◦C for 72 h. The experiments were conducted in triplicate, the diameter of the inhibition zone were measured and the results were reported as mean ± SD.

2.5 Formulation of ofloxacin (0.3%, w/v)-loaded carboxymethyl gum katira-chitosan polyelectrolyte ophthalmic nanosuspension

The optimized batch (30 ml) of ofloxacin (0.13% w/v)-loaded carboxymethyl gum katira nanoparticle was lyophilllized in sterile aqueous medium using mannitol (0.65 gm) as cryoprotectant in laboratory model freeze dryer (Alpha 2-4 LD, Martin Christ, Germany) at 0.0010 mbar, -80^{o}C for 24h. The ophthalmic nanosuspension was prepared by reconstituting aseptically, the lyophilized powder with sterile water (13ml) to give Ofloxacin (0.3%, w/v) ophthalmic nanosuspension. The ophthalmic nanosuspension so obtained was characterized for particle size using particle size analyzer (Zetasizer Nano ZS90, Malvern UK)

2.6. In vitro corneal permeation study

Corneal permeation characteristics of ofloxacin (0.3%, w/v) ophthalmic nanosuspension so prepared was evaluated comparatively with the conventional commercial ophthalmic ofloxacin (0.3%, w/v) solution (Oflox®, Cipla Ltd., India) using isolated porcine cornea.[22] Fresh eyeball of pig was obtained immediately after slaughtering from the local butcher shop (Hisar, India) and transported to the laboratory in cold normal saline within an hour. The cornea was excised carefully along with 3-4 mm of scleral tissue and washed properly with normal saline until free from proteins. Isolated cornea was clamped between the donor and receptor compartments of modified Franz diffusion cell with endothelial and epithelial sides facing the

receptor and donor compartments respectively. The receptor compartment contained 11.5 ml of freshly prepared Ringer bicarbonate solution maintained at 35 ± 0.5°C under magnetic stirring. The area available for corneal permeation was 0.95 cm^2. One milliliter of test formulation was placed in the donor compartment over the cornea. An aliquot of 1 ml of the sample was withdrawn from receptor compartment at regular interval and analyzed spectrophotometerically at 290 nm. The study was conducted employing paired corneas i.e., one cornea of the animal was used for the permeation study of nanosuspension formulation and the contralateral cornea was used for conventional commercial ofloxacin solution. Corneal hydration levels were determined by removing the scleral tissue from the cornea at the end of experiment and weighing followed by dehydration by overnight soaking in methanol and drying in an oven at 90°C and weighing again.

2.7 Corneal toxicity

Corneal toxicity of formulated ofloxacin (0.3%, w/v) ophthalmic nanosuspension was evaluated by incubating freshly excised porcine corneas with the formulation at 35°C for 1h, followed by washing with phosphate buffer saline and fixing with formaline (8%, w/w) solution. The tissue was later on dehydrated with an alcohol gradient, put in melted paraffin and solidified in block form. Cross sections of corneal tissue (<1 μm) were cut stained with hematoxyline and eosine, blinded and observed under microscope. Cross sections of corneas incubated with phosphate buffer saline (negative control) and sodium dodecyl sulfate, 0.1%, w/v (positive control) were prepared in the same manner.

3. Results and discussion

Carboxymethylation of polysaccharides is based on the William synthesis[23] in which the polysaccharide alkoxide is reacted with monochloroacetic acid and the primary and secondary alcohol groups are substituted by carboxymethyl group. Carboxymethyl gum katira prepared in this study was found to be white in color, odorless. The average yield of the product was found to be 64%. The degree of carboxymethyl substitution as determined by classical acid wash method was found to be 0.6.

Fig 1 shows the FTIR spectra of gum katira and carboxymethyl gum katira in the frequency range of 4000-400 cm^{-1}. The spectra of gum katira shows a broad absorption band at 3432 cm^{-1} due to presence of hydroxyl groups. The peak exhibited at 2926 cm^{-1} can be attributed to C-H stretching of alkane. The peaks at 2370 cm^{-1} and 2345 cm^{-1} can be ascribed to –CH stretch of alkene, while peak at 1600 cm^{-1} is due to the stretching vibrations of carbonyl of (-C=O) aldehydes and ketones. The O-H bending vibrations appear at 1443 cm^{-1}.The peaks appearing at 1155 cm^{-1} and 865 cm^{-1} can be ascribed to(C-O-C) stretching of ether group and bending vibration of =CH group of alkene, respectively.

The spectra of carboxymethyl gum katira shows broad band at 3430 cm^{-1} due to OH stretching of alcohols. The peaks exhibited at 2927 cm^{-1} can be attributed to C-H stretching of alkane. Peak appearing at 1734 cm^{-1} is due to stretching vibration of carbonyl (-C=O) of aldehydes and ketones. The new band at 1406 cm^{-1} was assigned to the asymmetrical and symmetrical stretching vibrations of carboxylate anion (-COO-) while the band at 1618 cm^{-1} was a characteristics of the $–CH_2$ scissoring in the carboxymethyl group. The –C-OH stretching of alcohols and –C-O-C- stretching of ether and group appeared at 1254 cm^{-1} and 1052 cm^{-1} respectively.

Fig 2 (a), (b) and (c) display the differential scanning calorimetric, thermogravimetric and first derivative curves of gum katira and carboxymethyl gum katira. The DSC curve of gum katira shows a broad endotherm at 63.20 ^{o}C, while the DSC curve of carboxymethyl gum katira shows a broad endotherm at 116.15 ^{o}C. The shift in endothermic transition temperature indicates modification of gum katira.

Table 1 presents the thermal degradation characteristics of gum katira and carboxymethyl gum katira as observed from their thermogravimetric (Fig. 2b) and first derivative curve (Fig. 2c). The thermal degradation of polymers shows several weight loss steps which can be attributed to evaporation of water and degradation of polymer. The DTG curve of gum katira shows four stages of degradation. The weight loss in the first stage is mainly due to loss of physical absorbed water and removal of structural water. The second stage of decomposition which is characterized by weight loss of 30.78% can be attributed to the depolymerization and rupture of C-O and C-C bonds of the saccharide ring. The third and fourth stage of degradation is due to advanced degradation of polymeric chain. The thermal degradation curve of carboxymethyl gum katira exhibited two stages of degradation. The first one with the weight loss of 17.50% can be ascribed to the loss of water. The second stage of degradation with weight loss of 5.56% is due to depolymerization and degradation of polymeric chain. Further, it can be observed that at the end of the degradation study at 600^{o} C the residual mass of 9.98% and 76.94% was left for gum katira and carboxymethyl gum katira respectively. The results thus point to the improvement in thermal stability of gum katira on carboxymethylation.

Fig. 3 (a) and (b) portrays the X-ray diffraction spectra of gum katira and carboxymethyl gum katira. The X-ray diffraction pattern of gum katira is typical of amorphous material with no sharp peak while the difractogram of carboxymethyl gum katira shows characteristics diffraction peaks appearing at 16.87^{o}, 28.14^{o}, 29.54^{o}, 32.34^{o}, 33.50^{o}, 36.30^{o}, 37.38^{o}, 40.42^{o}, 41.14^{o}, 43.74^{o}, 45.05^{o}, 54.93^{o}, 57.33^{o}, 75.20^{o} (2θ). Thus appearance of characteristics sharp peaks with higher intensity in the diffraction pattern of carboxymethyl gum katira indicates the increase in degree of crystallinity of gum katira on carboxymethylation. Earlier reports on carboxymethylation of

amylopectin[24], xanthan[12] and gum kondagogu[10] also revealed the increase in degree of crystallinity of polysaccharides on their carboxymethylation.

Fig. 4 (a-d) displays the scanning electron micrographs showing the shape and surface morphology. The micrographs of gum katira (Fig. 4 a & b) shows the presence of thin flakes of gum katira with smooth surface while the micrographs of carboxymethyl gum katira (Fig. 4 c and d) shows the presence of polyhedral shaped particles with rough sharp edged surface. The surface morphology of carboxymethyl gum katira corroborates with the result of X-ray diffraction study which showed increased crystallinity of craboxytmethyl gum katira.

Fig. 5 compares the viscosity of aqueous dispersion (2%, w/v) of gum katira and carboxymethyl gum katira. It can be inferred from the plot that carboxymethylation of gum katira results in significant fall in viscosity of gum katira. Earlier studies also reported that carboxymethylation of carbohydrate polymers leads to decrease in viscosity. The decrease in viscosity due to carboxymethylation can be explained by the fact that carboxymethylation imparts anionic character on the carbohydrate backbone chain. The columbic repulsion between the polymeric chain leads to decrease in viscosity[25].

Caboxymethyl functionalization of gum katira renders it anioinic in nature which makes it suitable for preparation of ionically gelled particulate systems[26]. It was observed during preliminary trials that carboxymethyl gum katira interacts with cationic chitosan to form polyelectrolyte complexes, which prompted us to explore these polyelectrolyte complexes for drug delivery applications. Further, it was found that varying the concentration of carboxymethyl gum katira and chitosan affected the particle size of polyelectrolyte complex, yielding

302 precipitates to the colloidal solution. The conventional approach of varying one-factor- at- a-
303 time (OFAT) is time consuming, uneconomical and just gives the workable solutions. In contrast
304 systematic approach of formulation development based on the Quality by design (QbD)
305 paradigm which provides product with best possible characteristics in an economical way has
306 become quite popular. Thus, in the present study the principles of Design of Experiment (DOE)
307 were employed to study the interaction between carboxymethyl gum katira and chitosan. The
308 interaction between the two factors was optimized employing 2-factor, 3-level central composite
309 experimental design to prepare polyelectrolyte complex particles in the nanometric ranges. A
310 total of thirteen batches were prepared as per the face-centered cubic design with α=1, studying
311 the effect of concentrations of carboxymethyl gum katira and chitosan including quintuplicate
312 studies at the center point (0, 0). [27]

313 Table 2 presents the results of particle size and entrapment efficiency of thirteen batches
314 of carboxymethyl gum katira-chitosan polyelectrolyte nanoparticles prepared as per the design
315 protocol.. The results of the study were subjected to model fitting in various polynomial models.
316 It was observed that the response particle size (Y_1) fitted best into quadratic response surface
317 model with backward elimination after square root transformation of the data, while with
318 response entrapment efficiency (Y_2) was found to fit best into the quadratic response surface
319 model. The polynomial equations expressing the relationship between the formulation variables
320 and response variables for the responses Y_1 and Y_2 in terms of coded values are as follows:-

321 $$Y_1(nm) = 16.29 + 1.06X_1 + 4.96X_2 + 3.94{X_2}^2 \quad \ldots\ldots\ldots\ldots(3)$$

322 $$Y_2\ (\%) = 82.97 - 1.23X_1 + 17.10X_2 + 3.54X_1X_2 + 1.43{X_1}^2 - 13.30{X_2}^2 \ldots(4)$$

323

Table 3 shows the results of ANOVA analysis on the polynomial models. The results revealed that the developed polynomial models are significant ($P<0.05$) with non significant lack of fit ($P>0.05$). The higher values of R^2 and the reasonably good agreement between the adjusted R^2 and predicted R^2 values indicate model reliability. In addition the higher values of adequate precision (> 4) show adequate signal and indicate that the developed model are fit to navigate the design space.

Fig 6 (a) illustrates the combined effect of concentrations of the caboxymethyl gum katira and chitosan on the particle size of carboxymethyl gum katira-chitosan polyelectrolyte nanoparticles. It can be inferred from the plot that the effect of carboxymethyl gum katira concentration is more prominent than the effect of chitosan. As the concentration of carboxymethyl gum katira is increased from 0.1-0.4% the particle size increases significantly. This increase in size can be explained by the fact that increasing the concentration of carboxymethyl gum katira increases the viscosity of carboxymethyl gum katira solution leading to aggregation of nanoparticles and/or inadequate interaction between chitosan and viscous carboxymethyl gum katira.

Fig 6 (b) displays the combined effect of concentrations of carboxymethyl gum katira and chitosan on the entrapment efficiency of ofloxacin. The effect of carboxymethyl gum katira concentration on entrapment of ofloxacin is more pronounced than the chitosan. This effect of carboxymethyl gum katira concentration on entrapment efficiency can be explained similar to its effect on particle size. The ofloxacin containing carboxymethyl gum katira solution of higher viscosity (i.e higher concentration), prevents the leaching out of ofloxacin from the interacting gel phase into the bulk of solution more efficiently as compared to the carboxymethyl gum katira solution of lower viscosity (i.e lower concentration).

The preparation of carboxymethyl gum katira-chitosan polyelectrolyte nanoparticles with desirable particle size and entrapment efficiency was accomplished by employing numerical optimization tool of design expert software. The optimization of concentration of carboxymethyl gum katira (X_1) and chitosan (X_2) was done with constraints for minimum particle size and maximum entrapment efficiency. The optimal calculated parameters were concentration of carboxymethyl gum katira (X_1) 0.26 % and concentration of chitosan (X_2) 0.03 %. The optimized batch of carboxymethyl gum katira-chitosan polyelectrolyte nanoparticles had a particle size of 269 nm (Predicted 242.5 nm), PdI of 0.236 and entrapment efficiency of ofloxacin of 83.65% (Predicted 86.48%). This batch was further characterized for morphology and *in vitro* release behavior.

The morphology of optimized batch of ofloxacin nanoparticles was visualized using Transmission electron microscopy (Fig 7). The transmission electron micrograph shows the presence of ovoid nanoaggregates.

Fig 8 shows the *in-vitro* release profile of ofloxacin from optimized batch of carboxymethyl gum katira-chitosan polyelectrolyte nanosuspension using dialysis sac method. It can be observed that the polyelectrolyte nanoparticles showed a burst release of the drug with about 20% of the drug getting released within first 30 min. This burst release can be attributed to the faster diffusion of unentrapped ofloxacin present in the nanosuspension and ofloxacin present on the surface of nanoparticles. Further about 46% of the ofloxacin was released in 2h followed by slower release of the drug sustained over 24 h. A total of 92% of the drug was released during the study period of 24h.To study the limiting effect of dialysis membrane in vitro release study of aqueous ofloxacin solution of equivalent concentration was also carried out, which relased the entire drug within 2 h of the study. To determine the kinetics and mechanism of release the release rate data was fitted into various kinetic models. The value of R^2 was found to be 0.467, 0.923, 0.934 and 0.826 for zero-order, first-order, Higuchi's square root and Korsemeyer-Peppas models. Thus, the release of ofloxacin from the polyelectrolyte nanosuspension followed the Higuchi's square-root kinetics. Further, the value of '*n*', the release exponent of Korsemeyer-

Peppas model was found to be 4.248 (n>1), indicating the mechanism of release is Super Case-II transport.

Table 4 compares the results of anti-bacterial activity of ofloxacin-loaded carboxymethyl gum katira–chitosan nanoparticles with the ofloxacin solution of equivalent concentration against *Escherichia coli*, *Staphylococcus aureus, Pseudomonas aeruginosa.* The results show that optimized batch of ofloxacin-loaded nanoparticles produced zones of inhibition comparable to ofloxacin solution. Chitosan is reported to exhibit antibacterial activity[28]. However, the results of carboxymethyl gum katira-chitosan polyelectrolyte nanoparticles (blank control) did not show any significant zone of inhibition indicating that the antibacterial activity of ofloxacin-loaded polyelectrolyte nanosuspension is not due to the presence of chitosan in the nanosuspension. Further, the optimized batch had 83.65% of the drug entrapped in the nanoparticles but it did not show any adverse effect on the antibacterial activity of ofloxacin.

The optimized batch of ofloxacin- loaded polyelectrolyte nanosuspension was lyophilized using mannitol as cryoprotectant, which also served as tonicity modifier. The powder on reconstitution with sterile water provided ofloxacin (0.3%, w/v) ophthalmic nanosuspension. However, there was no significant affect of lyophilization on the particle size of reconstituted ophthalmic nanosuspension as it had the particle size of 282 nm with PdI of 0.342.

Table 5 and Fig. 9 presents the results of corneal permeation study of ofloxacin from the formulated ofloxacin (0.3%,w/v) polyelectrolyte nanosuspension and commercial ofloxacin 0.3%, w/v (Oflox®) ophthalmic solution across porcine cornea. A slightly higher apparent corneal permeability (Papp) was observed from the nanosuspension formulation as compared to the conventional solution. Higher corneal permeability of nanosuspensions was earlier attributed to endocytic uptake of nanoparticles.[29] The commercial formulation contained benzalkonium chloride as preservative, which have earlier been reported to enhance the corneal permeation of ofloxacin.[22] Even though no preservative was added in the polyelectrolyte nanosuspension, it provided higher corneal permeability of ofloxacin. Further, it is expected that during *in vivo* use ophalmic nanosuspension would be retained in the '*cul-de-sac*' providing sustained release of ofloxacin over aolonged period of time.

The corneal hydration levels of the corneas employed in the permeation studies indicate the integrity of cornea, normal corneal hydration levels are reported to be 75-80%.[30] Since the corneal hydration levels in the present study are within the limits, the corneal integrity was not affected. Further, the effect of formulated ofloxacin polyelectrolyte ophthalmic nanosuspension on corneal integrity was studied by conducting histological studies. Fig.10 a, b, c &d displays the cross sections of corneas incubated with SDS (Control irritant), phosphate buffer saline (control non-irritant), formulated ofloxacin polyelectrolyte nanosuspension and commercial ofloxacin ophthalmic solution. The cross sections of cornea treated with SDS show separation of superficial corneal epithelium and widening of intercellular spaces, while the corneas treated with phosphate buffer saline had a well maintained epithelium and stroma. The cross sections of corneas treated with formulated ophthalmic nanosuspension and commercial solution were also similar to the corneas treated with phosphate buffer saline. The results of histological studies confirm the corneal biocompatibility of ofloxacin-loaded carboxymethyl gum katira-chitosan polyelectrolyte nanosuspension.

Conclusion

Carboxymethyl modification of gum katira was carried out with the objective to modify its physicochemical properties. Carboxymethylation was found to reduce its viscosity, improve dispersibility, increase thermal stability and impart anionic character on the carbohydrate backbone. The interaction between the anionic carboxymethyl gum katira and cationic chitosan was optimized to prepare polyelectrolyte complex nanoparticles having optimal size and entrapment using ofloxacin as a model drug. The optimized batch of nanoparticles was employed for preparing ophthalmic nanosuspension. On comparative evaluation the polyelectrolyte nanosuspension was found to provide higher *in vitro* corneal permeability of ofloxacin across

isolated porcine cornea than the ophthalmic solution. Further, the results of histological studies of corneas treated with polyelectrolyte nanosuspension indicated its corneal biocompatibility. The results of present study indicate potential usefulness of polyelectrolyte complexes of carboxymethyl gum katira and chitosan in ophthalmic drug delivery. However, further *in vitro* and *in vivo* studies are required to establish its use in pharmaceutical systems.

Acknowledgements

The authors express gratitude to University Grant Commission, New Delhi for providing financial assistance to Mr Minkal under SAP Scheme vide reference no. F.3-25/2012 (SAP-II) and to the Coordinator DST-FIST, Department of Pharmaceutical Sciences and Material Science Laboratory, Department of Physics, GJUS &T, Hisar for providing the facilities for particle size analysis and thermal analysis, respectively.

References

1. T.R. Bhardwaj, M. Kanwar, R. Lal, A. Gupta, *Drug. Dev. Ind. Pharm.* 2000, **26**, 1025-1038.

2. V. Rana, P. Rai, A. K. Tiwary, R. S. Singh, J. F. Kennedy, C. J. Knill, *Carbohydr. Polym.* 2011, **83,** 1031–1047

3. D.R. Biswal, R. P. Singh, *Carbohydr. Polym.* 2004, **57,** 379-387.

4. F. R. Abreu, S. P. Campana-Filho, *Polímeros,* 2005, **15,** 79–83.

5. T. Heinze, A. Koschella, *Macromol Symp,* 2005, **223,** 13–19.

6. G. Dodi, D. Hritcu and M. I. Popa, *Cellulose Chem. Technol.* 2011, **45 (3-4)**, 171-176.

7. D. N. Iqbal, E. A. Hussain and N. Naz, *Int J Pharm Bio Sci.* 2013, **4(4),** 305 – 316.

8. R. Huynh, F. Chaubet, J. Jozefonvicz, *Die Angew. Makromol. Chem.,* 1998, **254,** 61–65.

9. A. Kumar, S.Singh, M. Ahuja, *Int J Biol Macromol.* 2013, **53,** 114-121.

10. A. Kumar, M. Ahuja, *Carbohydr. Polym.* 2012, **90,** 637–643.

11. T.A. Charito., N. Naotsugu, B. Aristea, D.S. Alumanda, *Carbohydr. Polym.* 2012, **87,** 1810–1816.

12. M. Ahuja, A. Kumar, K. Singh, *Int. J. Bio. Macromol.* 2012, **51,** 1086–1090.

13. Wealth of India; CSIR: New Delhi, 1962; vol. 2, p 261.

14. K.R. Kirtikar, B.D. Basu. Blatter, E., Caius, J.F., Mahasker, K.S., Eds; Bishen Singh Mahendra Pal Singh: Dehradun, India, 1998; Vol 1, pp 214-215.

15. A. K. Ojha, D. Maiti, K. Chandra, S. Mondal, D. S. K. Roy, K. Ghosh and S. S. Islam *Carbohydr. Res.* 2008, **343,** 1222–1231.

16. B. Bharanirajaa, K. Jayaram Kumara, C.M. Prasada, A.K. Sen. *Int. J. Bio. Macromol.* 2011, **49,** 305–310.

17. I. Singh, P. Kumar, S. Kumar, V. Rana, *Yakugaku Zasshi,* 2010, **130 (9),** 1225-1231.

18. S. Maity, I. K. Sen, S.S. Islam, *Physica E* 2012, **45,** 130-134.

19. K.M. Narayana, *Ind. Drugs.* 1992, **29,** 404-407.

20. R.W. Eyler, E.D. Klug, F. Diephuis. *Anal. Chem.* 1947, **19(1),** 24-27.

21. M. Ahuja, A. S. Dhake, S. K. Sharma, D. K. Majumdar, *J. Microencapsul.* 2011, **28 (1),** 37-45.

22. M. Ahuja, G. Singh, D.K. Majumdar, *Sci. Pharm.* 2008, **76,** 505-514.

23. D. A. Silva, C.M.R. de. Paula, P.A.J. Feitosa, C.F.A. de. Brito, S. J. Maciel, C.B. H. Paula, *Carbohydr. Polym.* 2004, **58,** 163–171.

24. K. Thakur, M. Ahuja, A. Kumar, *Int. J. Bio. Macromol.* 2013, **62,** 25-29.

25. S. Maiti, S. Ray, B. Mandal, S. Sarkar, B. SA, *J. Microencapsul.,* 2007, **24(8),** 743-756.

26. A. Kumar, M. Ahuja, *Int. J. Bio. Macromol.* 2013*,* **62,** 80-84.

27. B.Singh, R. Kumar, N.Ahuja, *Crit. Rev. Therap. Drug Carrr. Sys*.2004, **22**, 27-105.

28.E.J. Rabea, M.E.T. Badawy, C.V.Stevens, G. Smagghe, W. Steurbaut , *Biomacomol.*2003,**4**, 1457-1465.

29.P. Calvo, M.J. Alonso, J.L. Vila-Jato, J.R.Robinson, *J Pharm Pharmcol*, 1996, **48,** 1147 -1152.

30. D.M. Maurice, M.V. Riley., ed. C.N. Graymore, Academic Press, London, 1970. pp. 6-16.

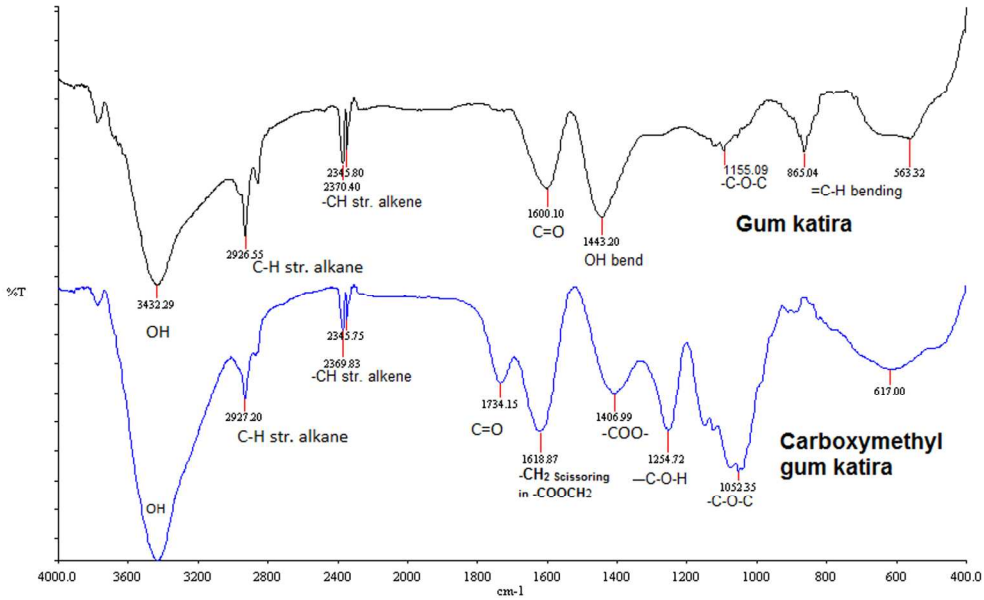

Fig. 1. FTIR Spectra of gum katira and carboxymethyl gum katira
229x138mm (300 x 300 DPI)

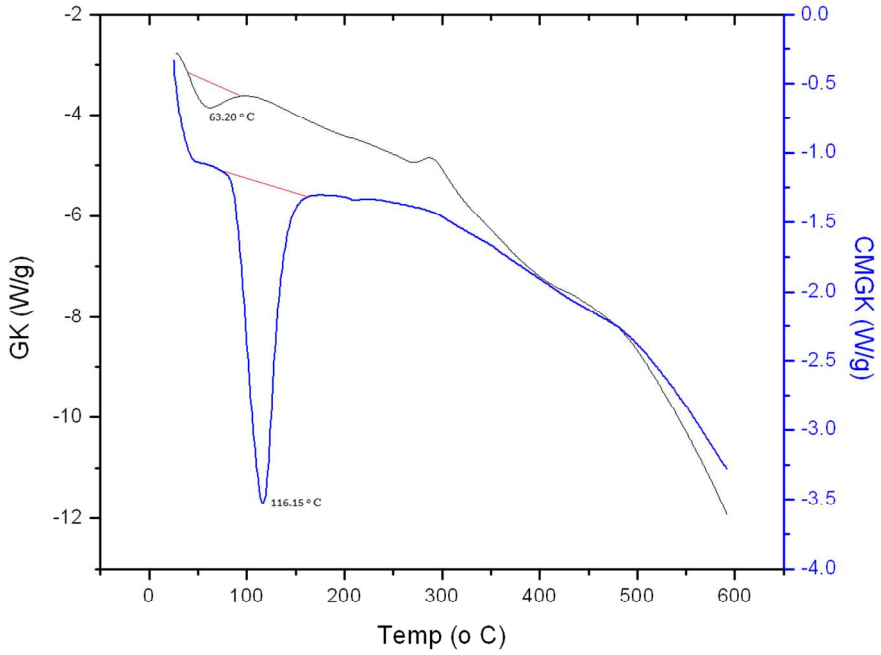

Fig. 2. DSC (a) curves of gum katira and carboxymethyl gum katira
111x86mm (300 x 300 DPI)

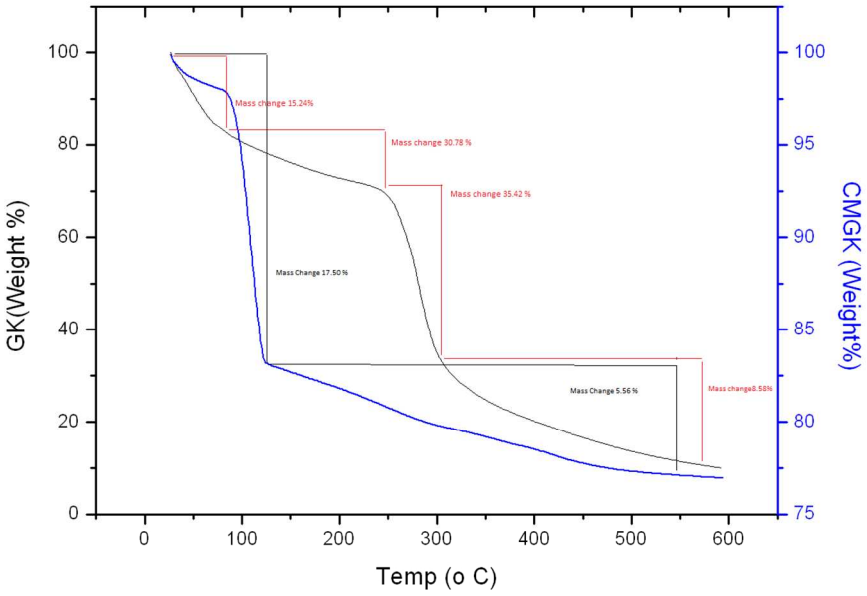

Fig. 2. TGA (b) curves of gum katira and carboxymethyl gum katira
118x83mm (300 x 300 DPI)

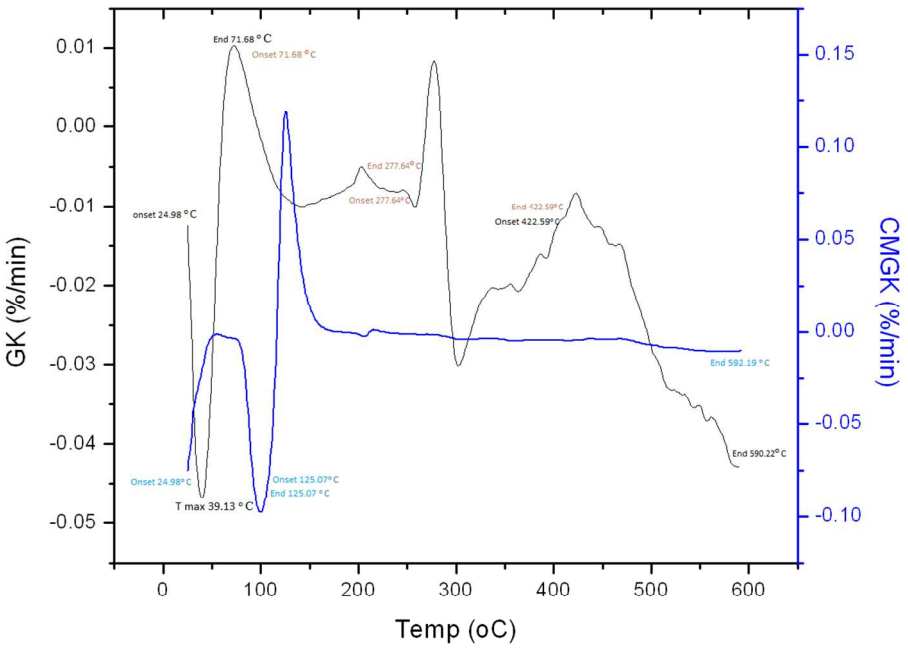

Fig. 2. DTG (c) curves of gum katira and carboxymethyl gum katira
111x86mm (300 x 300 DPI)

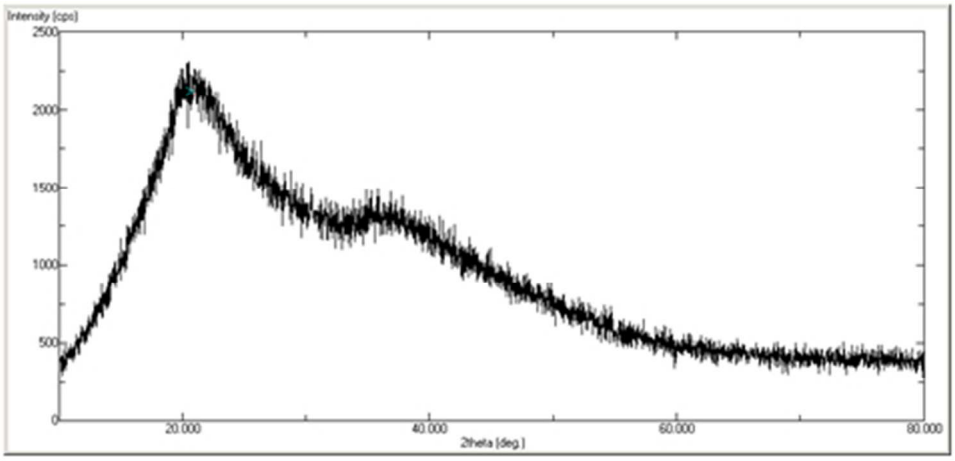

Fig. 3. X-ray diffractogram of gum katira (a)
128x62mm (96 x 96 DPI)

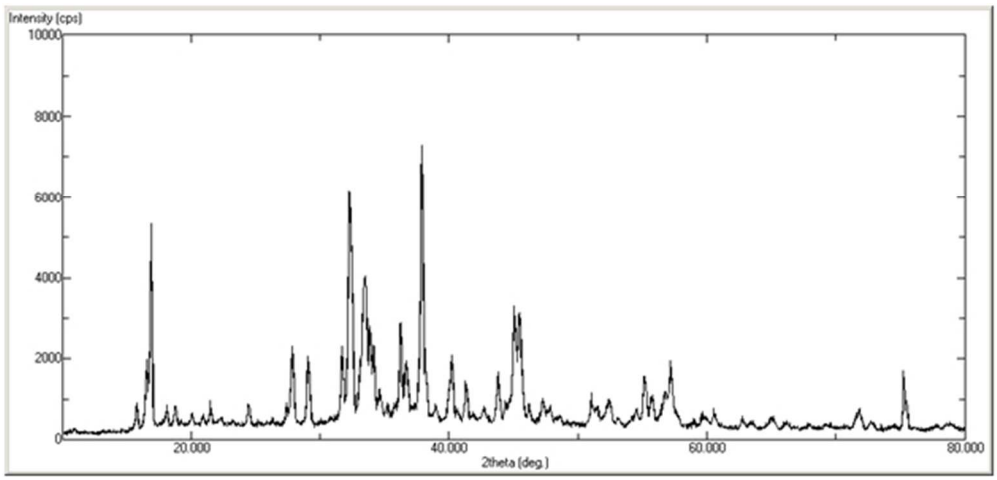

Fig. 3. X-ray diffractogram of carboxymethyl gum katira (b)
167x80mm (96 x 96 DPI)

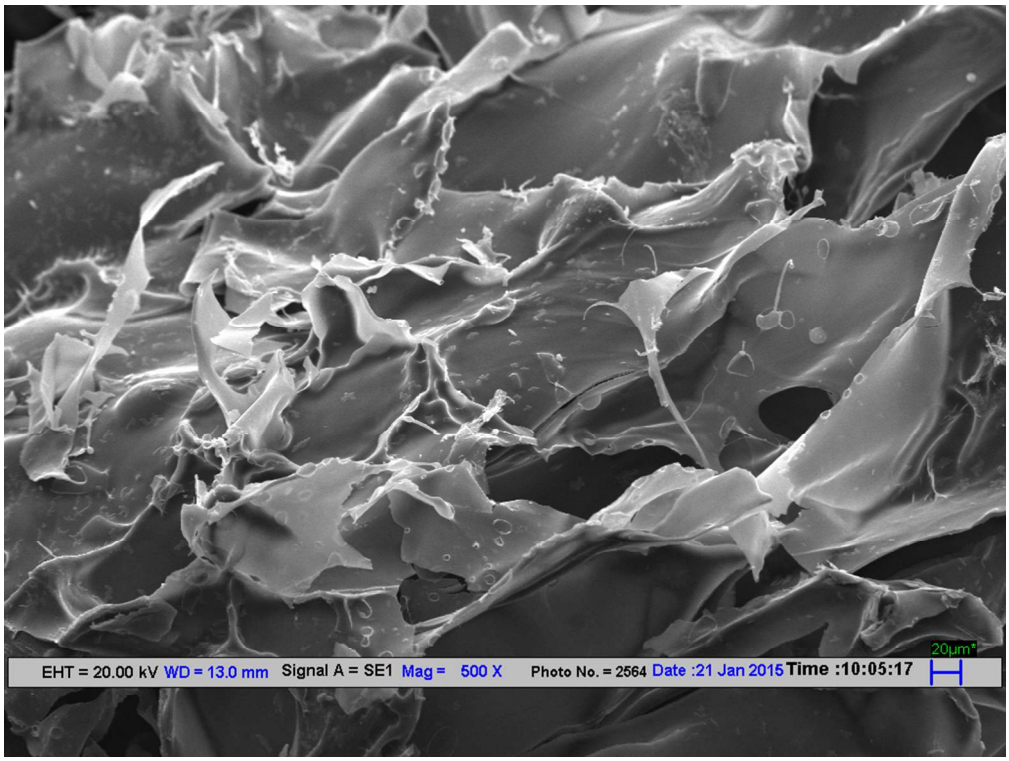

Fig. 4. Scanning electron micrograph of gum katira (a)

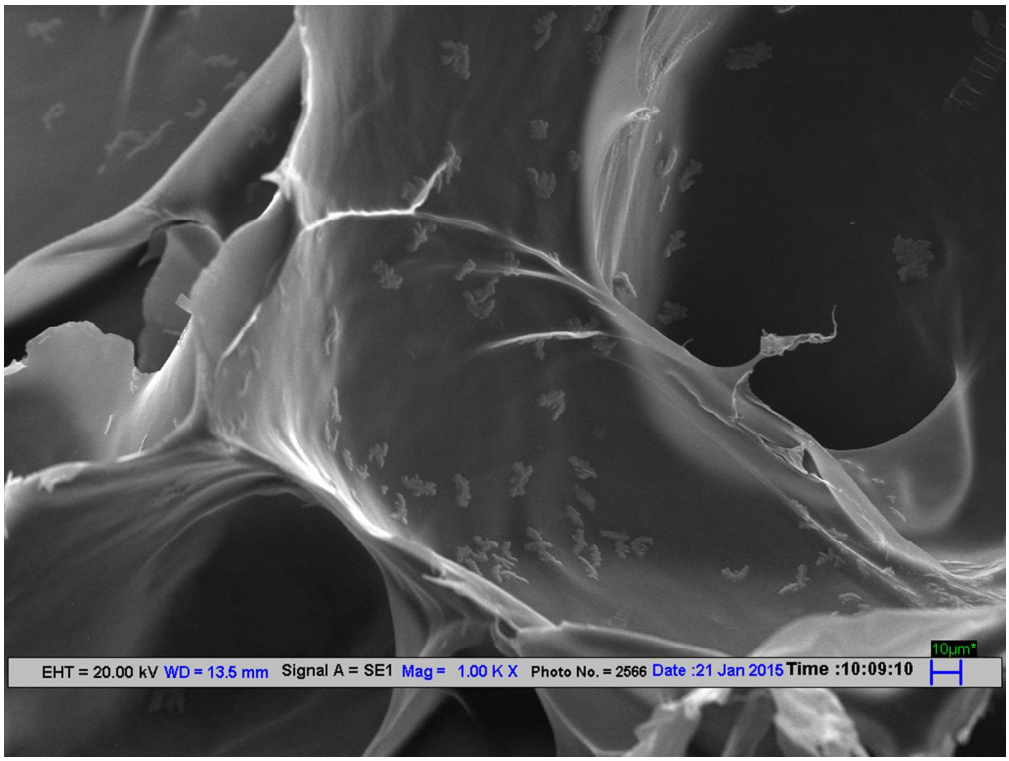

Fig. 4. Scanning electron micrograph of gum katira (b)

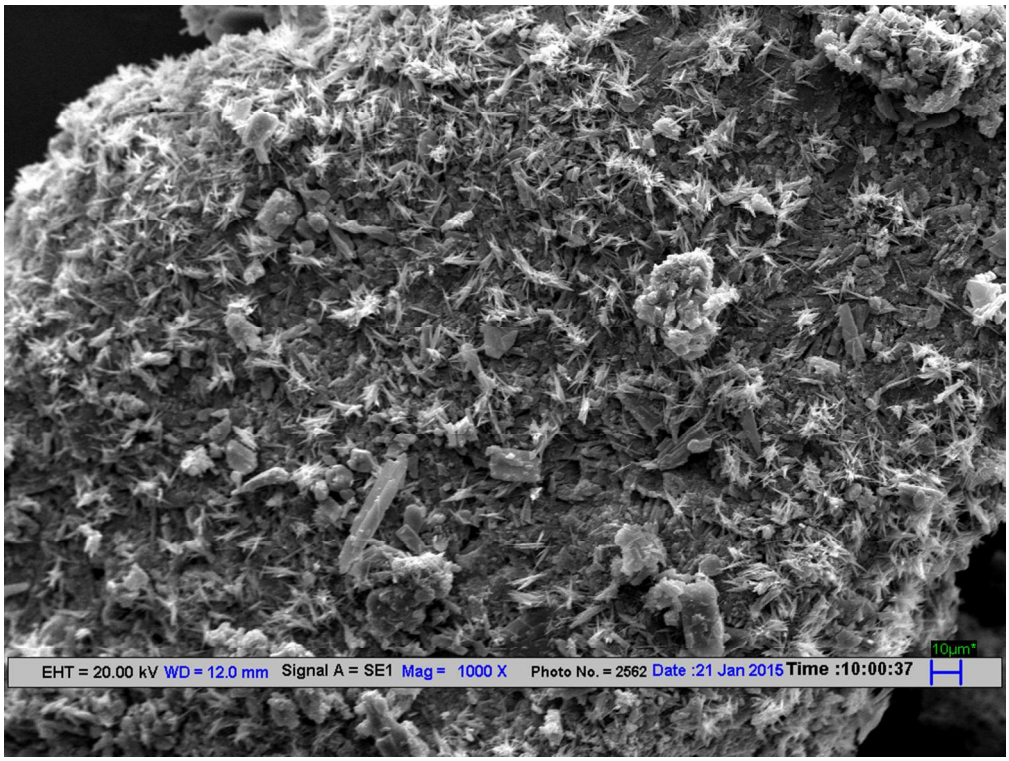

Fig. 4. Scanning electron micrograph of carboxymethyl gum katira (c)

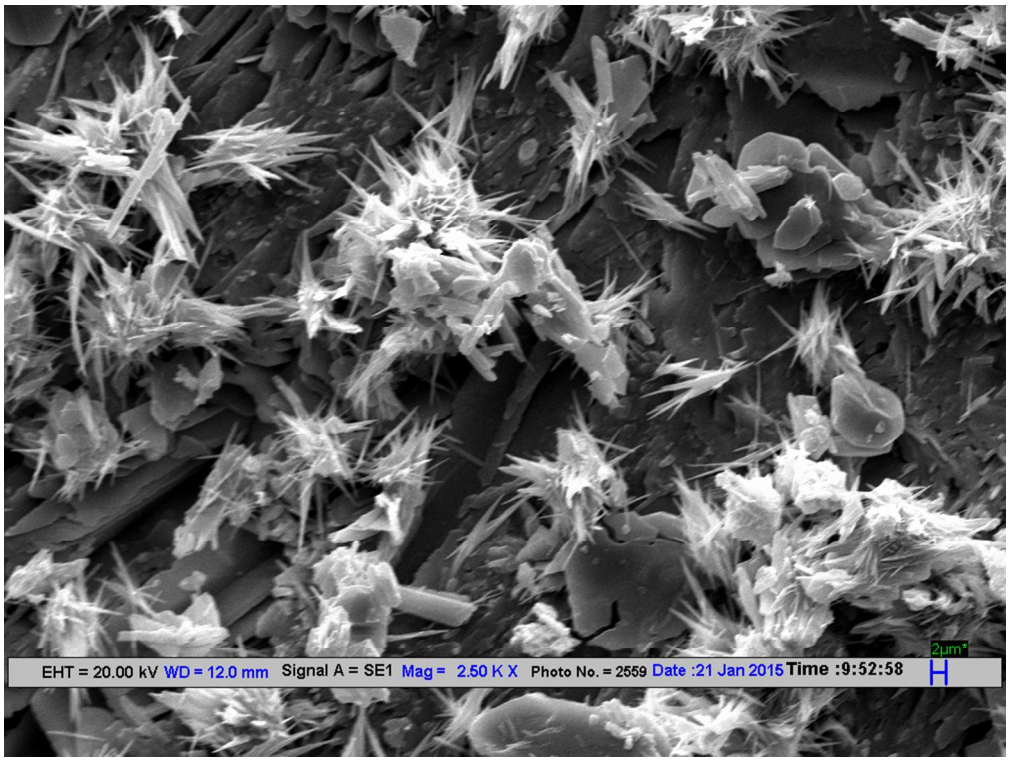

Fig. 4. Scanning electron micrograph of carboxymethyl gum katira (d)

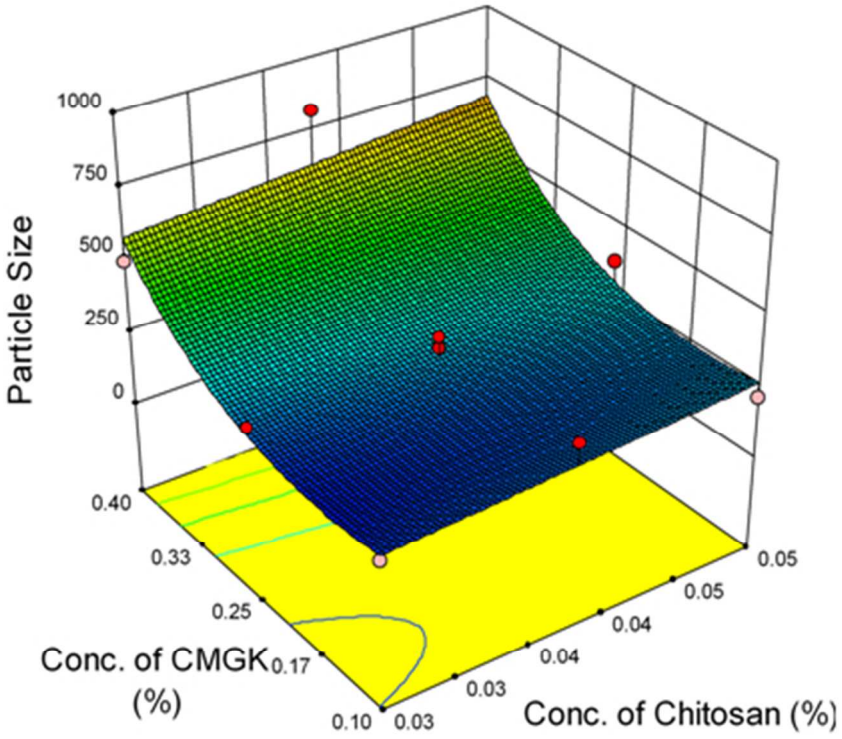

114x100mm (96 x 96 DPI)

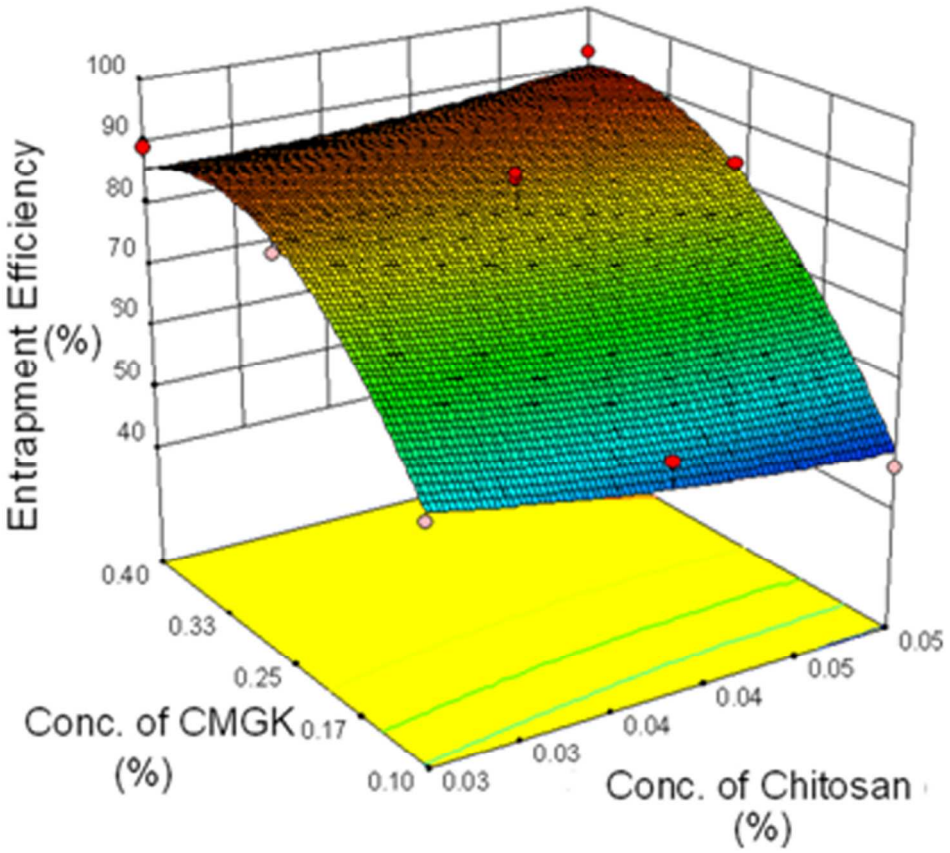

Fig. 6. Response surface plot showing the combined effect of concentrations of carboxymethyl gum katira and chitosan on (a) particle size (b) entrapment efficiency of nanoparticles.
99x87mm (300 x 300 DPI)

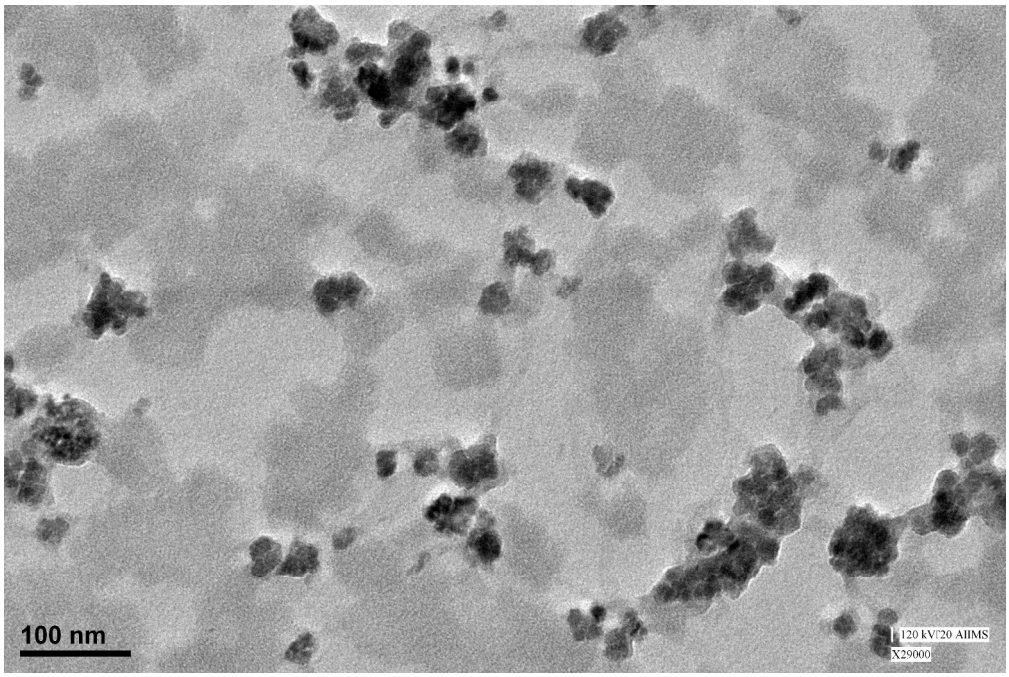

Fig. 7. Tranmission electron micrograph of optimized batch of caboxymethyl gum katira chitosan nanoparticles
1413x942mm (72 x 72 DPI)

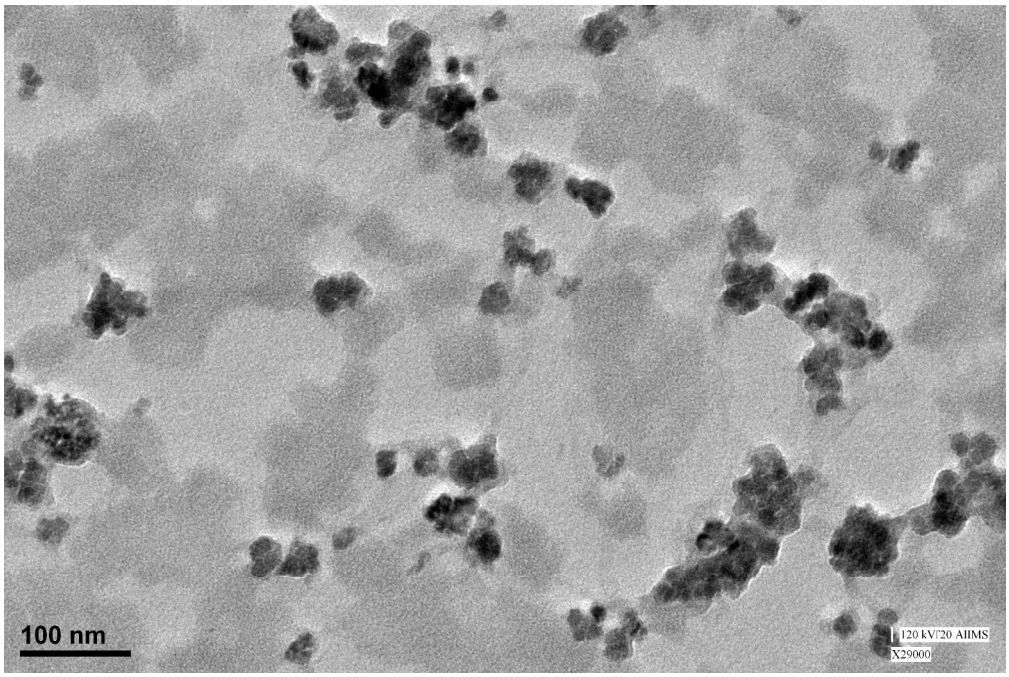

Fig. 7. Tranmission electron micrograph of optimized batch of caboxymethyl gum katira chitosan nanoparticles
1413x942mm (72 x 72 DPI)

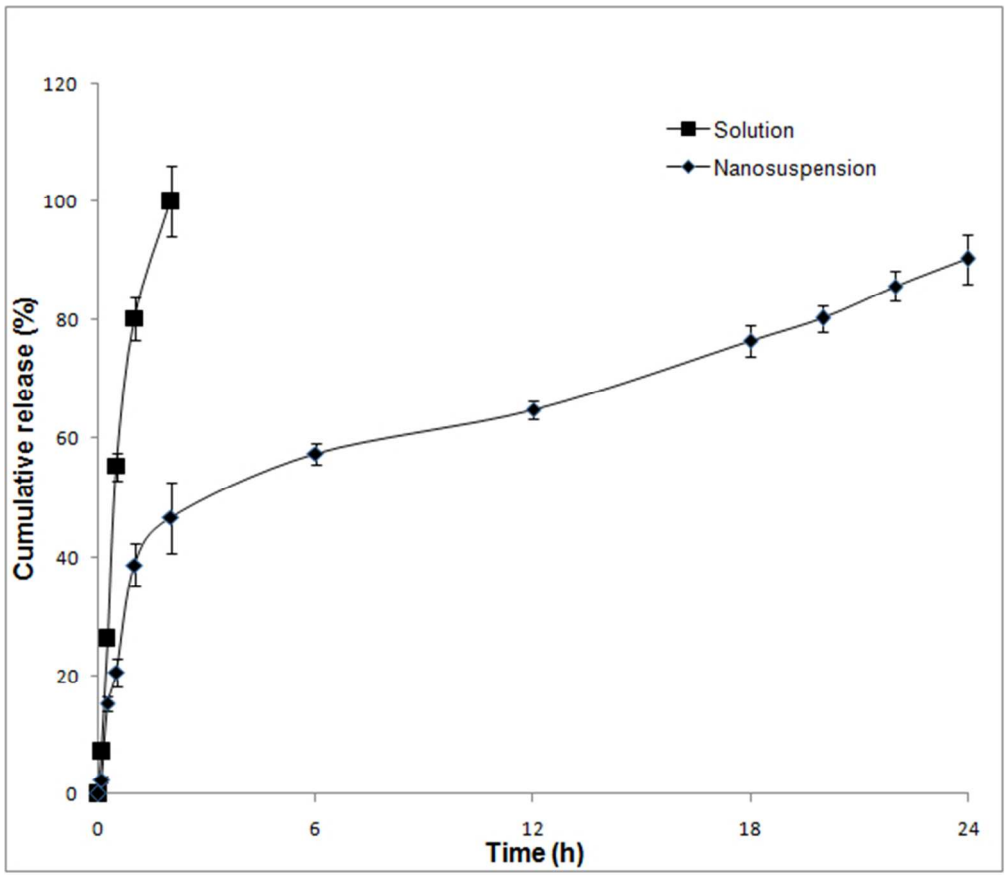

Fig. 8. Comparative in vitro release profile of nanosuspension and ofloxacin
161x139mm (96 x 96 DPI)

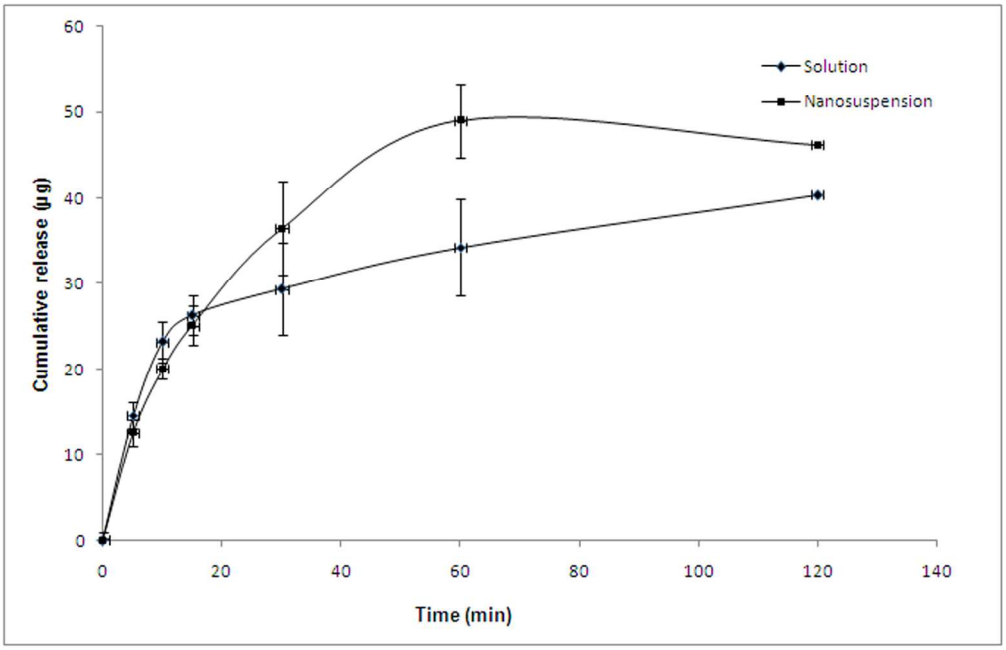

180x116mm (300 x 300 DPI)

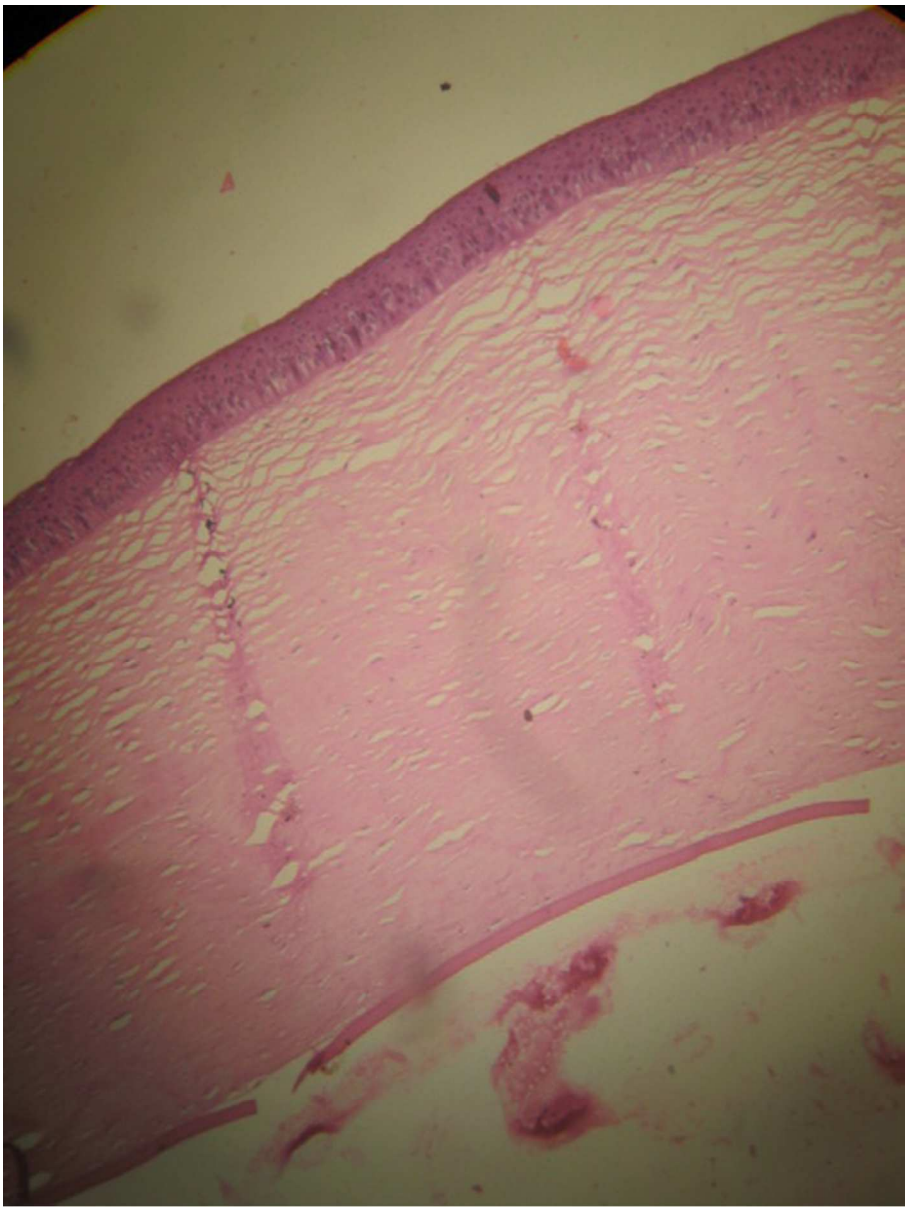

Fig. 10. Cross section of cornea treated with (a) SDS, (b) Phosphate buffer saline, (c) Ophthalamic nanosuspension, (d) Commercial eye drop
67x90mm (180 x 180 DPI)

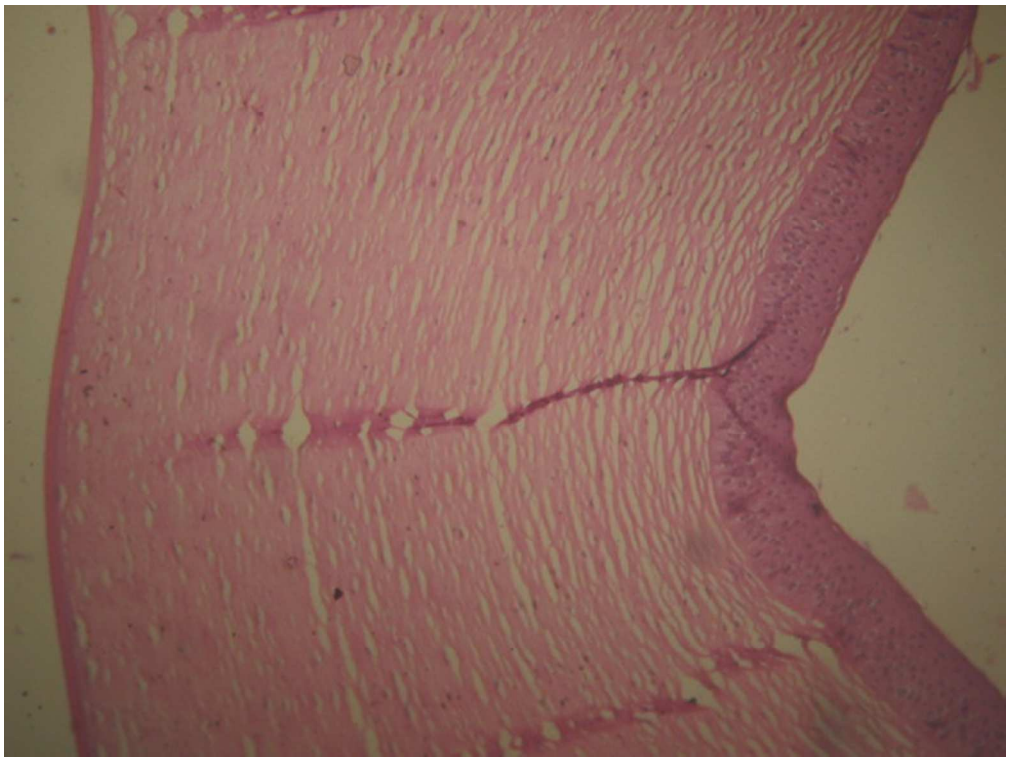

Fig. 10. Cross section of cornea treated with (a) SDS, (b) Phosphate buffer saline, (c) Ophthalamic nanosuspension, (d) Commercial eye drop
90x67mm (180 x 180 DPI)

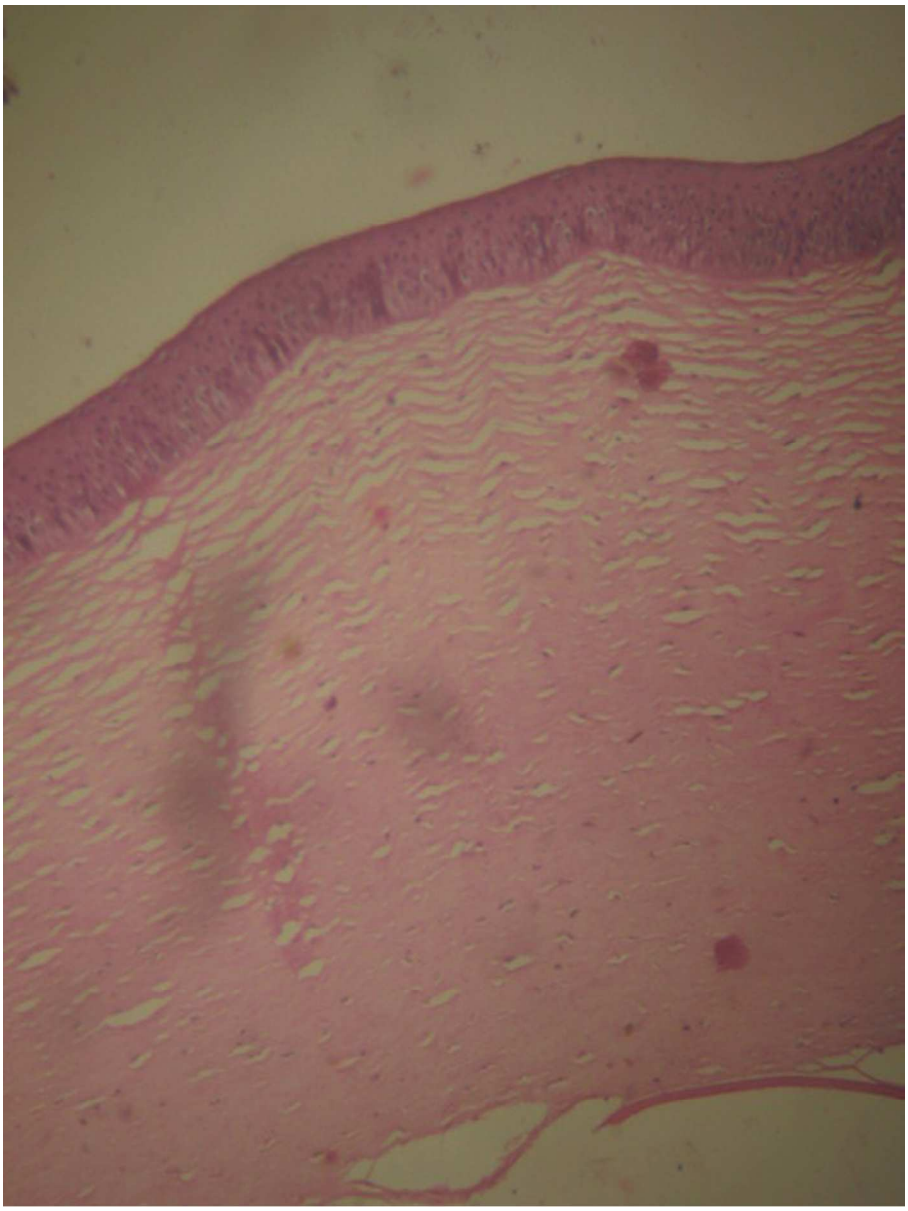

Fig. 10. Cross section of cornea treated with (a) SDS, (b) Phosphate buffer saline, (c) Ophthalamic nanosuspension, (d) Commercial eye drop
67x90mm (180 x 180 DPI)

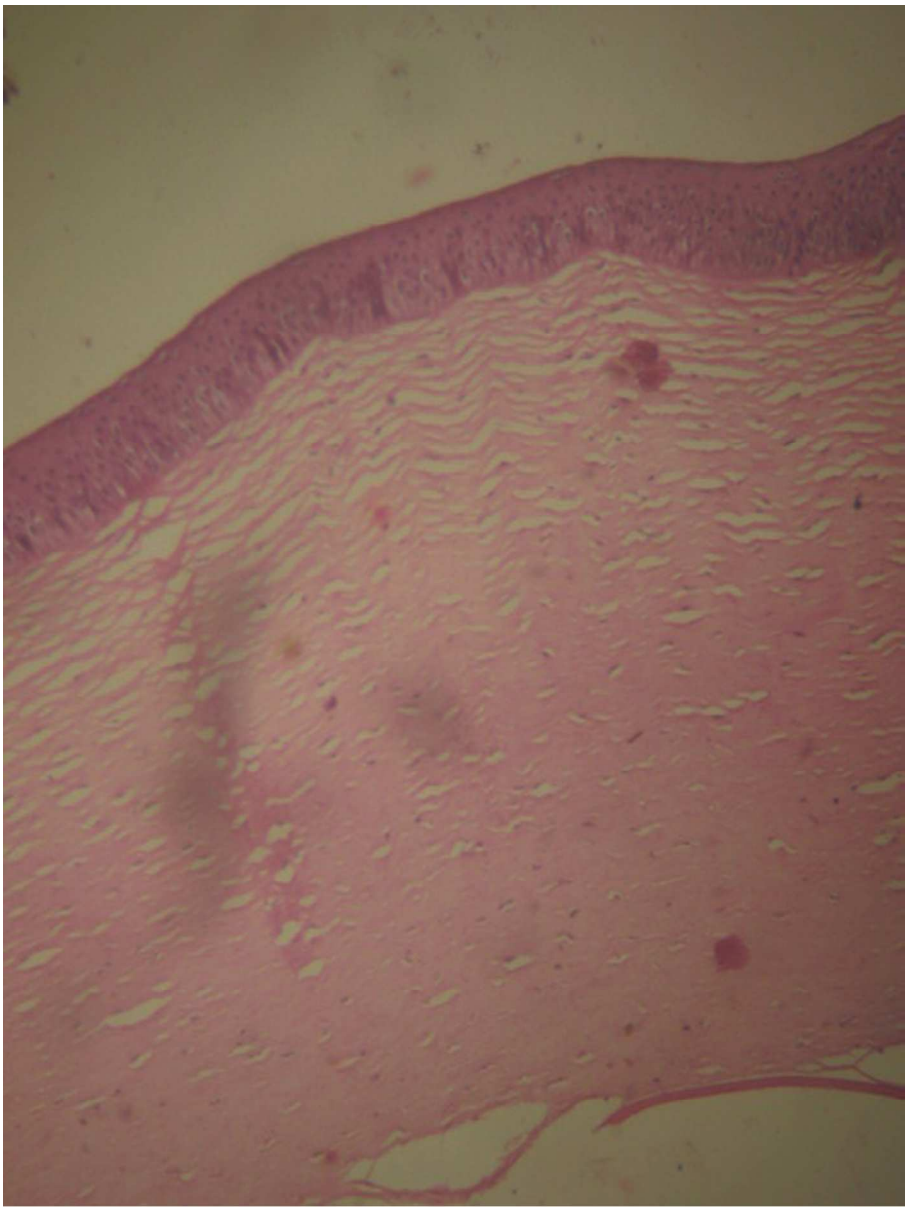

Fig. 10. Cross section of cornea treated with (a) SDS, (b) Phosphate buffer saline, (c) Ophthalamic nanosuspension, (d) Commercial eye drop
67x90mm (180 x 180 DPI)

Table 1 Thermogravimetric analysis of GK and CMGK

	T_{on} (^oC)	T_m (^oC)	T_{end} (^oC)	W_r (%)	T_{50} (^oC)	ΔW (%)
Gum katira	24.98	39.13	71.68	9.98	281	15.24
	71.68	203.44	277.64			30.78
	277.64	302.33	422.59			35.42
	422.59	-	590.22			8.58
Carboxymethyl gum katira	24.98	99.57	125.07	76.94	-	17.50
	125.07	-	592.19			5.56

Ton (onset temperature); Tm (maximum temperature); Tend (end temperature); Wr (residual weight); T50 (temperature at which weight remains 50 %); ΔW (weight change)

Table 2 Particle size and entrapment efficiency of various batches of carboxymethyl gum katira-chitosan polyelecrolyte nanoparticles.

Runs	Carboxymethyl gum katira (% w/v) (X_1)	Chitosan (% w/v) (X_2)	Particle Size (nm) (Y_1)	Entrapment Efficiency (%) (Y_2)	PdI
1	0.10 (-1)	0.03 (-1)	184.8	57.32	1.00
2	0.10 (-1)	0.04 (0)	308.1	56.77	0.52
3	0.10 (-1)	0.05 (1)	214.8	46.48	0.29
4	0.25 (0)	0.03 (-1)	260.9	83.65	1.00
5	0.25 (0)	0.04 (0)	216.0	87.86	0.57
6	0.25 (0)	0.04 (0)	174.7	88.91	1.00
7	0.25 (0)	0.04 (0)	236.0	81.17	0.63
8	0.25 (0)	0.04 (0)	292.4	79.21	0.44
9	0.25 (0)	0.04 (0)	329.9	79.08	0.69
10	0.25 (0)	0.05 (1)	373.0	83.75	0.62
11	0.40 (1)	0.03 (-1)	501.1	89.33	0.29
12	0.40 (1)	0.04 (0)	820.8	81.17	0.47
13	0.40 (1)	0.05 (1)	600.8	92.67	0.63

Table 3 Model Summary Statistics

Response factor	Model							Lack of fit	
	F-value	**Prob>F**	**R^2**	**Adj. R^2**	**Pred. R^2**	**Adeq Prec.**	**C.V (%)**	**F-value**	**Prob>F**
Y_1	19.19	0.0006	0.9320	0.8834	0.6280	12.293	6.38	1.17	0.4266
Y_2	12.73	0.0014	0.8093	0.7457	0.5699	9.378	12.77	1.72	0.3106

Table 4 Anti-microbial activity of ofloxacin-loaded carboxymethyl gum katira–chitosan nanoparticles

Sample	Diameter of Zone of Inhibition (mm)		
	Escherichia coli MTCC No. 40	*Staphylococcus aureus* MTCC No. 3160	*Pseudomonas aeruginosa* MTCC No. 424
Carboxymethyl gum katira–chitosan Nanoparticles	3.26 ± 0.25	2.54 ± 0.26	4.96 ± 0.13
Ofloxacin-loaded carboxymethyl gum katira–chitosan Nanoparticles	48.33 ± 4.16	46.66 ± 4.72	44.33 ± 7.76
Ofloxacin solution	52.66 ± 2.51	51.33 ± 2.08	50.66 ± 4.04

Values are mean ± SD (n=3)

Table 5 Corneal permeation characteristics of ofloxacin from ophthalmic nanosuspension and solution.

Formulation	Apparent permeability coefficient Papp × 10^{3} (cm/sec)	**Corneal Hydration (%)***
Ofloxacin ophthalmic nanosuspension	1.97	73.56 ± 0.56324
Ofloxacin ophthalmic solution	1.43	75.29 ± 0.96541

*Values are mean ± SD (n=3)

Figure Captions

Fig. 1. FTIR Spectra of gum katira and carboxymethyl gum katira

Fig. 2. DSC (a) TGA (b) and DTG (c) curves of gum katira and carboxymethyl gum katira

Fig. 3. X-ray diffractogram of gum katira (a) and carboxymethyl gum katira (b)

Fig. 4. Scanning electron micrograph of gum katira (a,b) and carboxymethyl gum katira (c,d)

Fig. 5. Rheological behavior of aqueous solutions of gum katira and carboxymethyl gum katira**.**

Fig. 6. Response surface plot showing the combined effect of concentrations of carboxymethyl gum katira and chitosan on (a) particle size (b) entrapment efficiency of nanoparticles.

Fig. 7. Tranmission electron micrograph of optimized batch of caboxymethyl gum katira chitosan nanoparticles

Fig. 8. Comparative *in vitro* release profile of nanosuspension and ofloxacin

Fig. 9. Corneal permeation profile of ofloxacin from ophthalamic nanosuspension and solution

Fig. 10. Cross section of cornea treated with (a) SDS, (b) Phosphate buffer saline, (c) Ophthalamic nanosuspension, (d) Commercial eye drop